

LONGITUDINAL SLIP IN ROLLING CONTACT

Uta Fügmann and Wolfgang Beier
Chemnitz University of Technology
GERMANY

ABSTRACT

In printing machines incorporating indirect printing technology, the image or pattern is first printed onto a blanket cylinder having an elastic rubber surface. Subsequently, the pattern is transferred to the substrate. When the surface of the blanket cylinder is covered with incompressible elastic material, a high tangential load develops at the blanket-substrate nip, which may either lead to longitudinal sliding of the mentioned printing element or cause tearing of the substrate. The described tangential load developing at the printing nip could be significantly reduced if the lining of the blanket included a compressible layer. The elastic material at the nip could now bear the tangential forces since the compressible layer could absorb them. In the printing result however, although quite minimal, the longitudinal slip can still be seen.

Study of the geometrical analysis and movements involved at the nip between the rigid and flexible contact presented an explanation.

For the geometric analysis of processes taking place at the nip, standard reverse kinematic transmission has been utilized. The flexible cylinder is taken as a fixed element while the rigid cylinder has been rolled as a planetary gear about a rolling contact. Both cylinders have bearer-to-bearer contact. Therefore they roll without any slip, ensuring a precise ratio of the angle of rotation. In order to achieve a defined contact pressure between the cylinder jackets, the projection above the bearer surfaces of the flexible and rigid cylinder have been measured, the sum of which is the metric pressure. When the rigid cylinder is rolled around the fixed flexible cylinder, each point on the surface of the rigid cylinder follows a path, the locus of which, when represented graphically forms an extended epicycloid.

The presented method of calculation, using the extended epicycloid apart from theoretically determining the slip, presents the ability to minimize the same.

INTRODUCTION

This paper examines the longitudinal slip between the rolling contact of two cylinders, using as example a rotary printing machine with indirect printing technology. In this machine, the rigid plate cylinder is mounted with a tensioned metal plate carrying the printing image which is transferred to a cylinder having an elastic printing surface and, finally, onto the substrate. The cylinder with the elastic surface, namely the blanket cylinder, carries a rubber blanket mounted under tension with help of clamps. The substrate (usually paper) is located on a steel cylinder, also known as the impression cylinder in sheet-fed presses (figure 6), or between two blanket cylinders in a web-fed press. Figure 1 shows the schematic of a printing unit in a rotary printing machine, in this case, a web offset printing press.

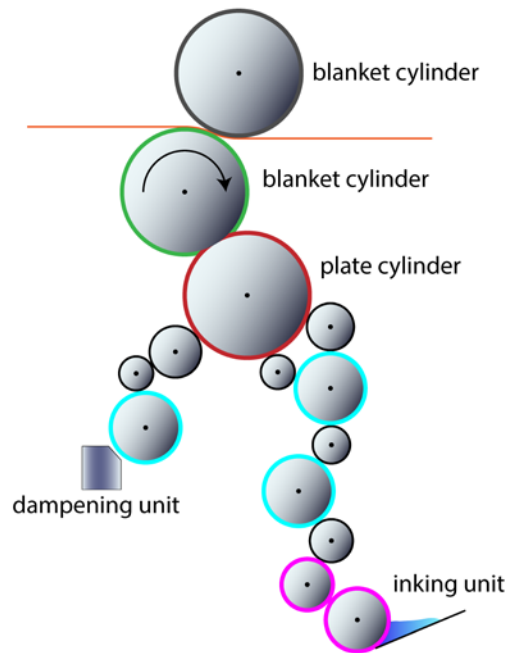
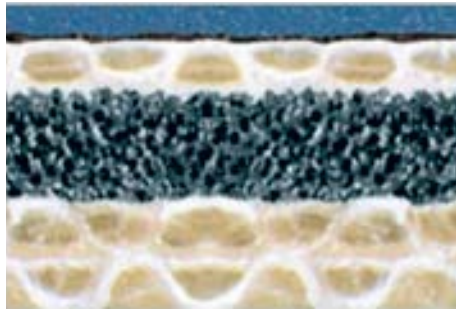


Figure 1 – Schematic of the printing unit of a web offset printing press (LaborMAN)

The blanket is made of an incompressible elastic material, which results in the development of high tangential stress in the contact zone (nip) between the cylinder surfaces. The resultant slip can lead to longitudinal sliding of the printing elements, causing increased wear of the printing plate or even tearing of the printing substrate. The high tangential stress at the contact zone can be reduced considerably by use of a compressible rubber blanket. In comparison to having only a solid rubber (volume), a compressible blanket contains an intermediate layer consisting of tiny gas bubbles to achieve compressibility. Therefore, the blanket does not react to the local compression with lateral displacement and does not yield to them as well. Figure 2 shows the cross-section of a commercially available compressible rubber blanket.



Face layer (elastomer)
 Upper fabric layer
 Compressible layer
 Double fabric layer

Figure 2 – Cross-section of a compressible blanket
 (Source: ContiTech Drucktücher)

Thus, the blanket exhibits distinctive anisotropic properties. It responds as elastic to the load in the vertical direction but presents a dimensionally stable surface for lateral forces. This lateral dimensional stability is created by the upper fabric layer and the integrated overlaying elastomer layer.

As described, this blanket should produce no slip while passing through the contact zone of two precisely synchronously driven cylinders. The conducted printing tests, however, showed a minimal but existent longitudinal slip.

This paper tries to find an explanation for the cause of the slip. First, the movements in the contact zone are analyzed geometrically and calculated in a number of examples in terms of hypothesis. Then a number of printing tests are carried out in order to verify the formulated hypothesis. Finally, the paper includes a critical evaluation of the slip calculation method.

HYPOTHESIS

To study the processes, the relative motion of a point located at the contact zone of a rigid and a flexible cylinder is considered. The flexible cylinder is mapped with a Cartesian coordinate system in such a way that the origin lies at the axis of this cylinder and rotates along with it. The system is more illustrative when the conventional kinematic conversion is applied in such a manner that the flexible cylinder (in this case the blanket cylinder) including the coordinate system is fixed, while the rigid cylinder (in this case the plate cylinder) orbits around it in the manner of a planetary gear (Fig. 3).

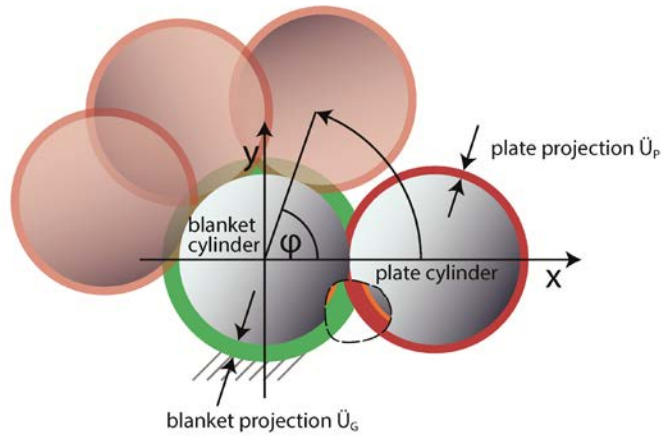


Figure 3 – Kinematic conversion of cylindrical motion

Precise rolling of the cylinders is ensured in the printing press by the end faces of the bearer rings which are firmly attached to the cylinders at both ends (Fig. 4).

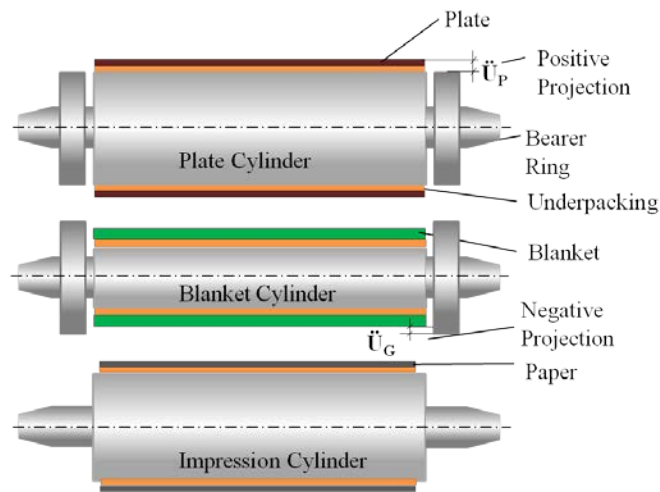


Figure 4 – Cylinder group with bearers

The bearer rings have a smooth cylindrical surface finish and are pressed together under stress, causing the cylinders to be under a definite pressure. Thus, the system ensures that the cylinders roll synchronously, since the small angular fluctuations caused by the driving gears are completely eliminated [1].

Ink transfer between the cylinders requires a defined compression between the rigid and the flexible cylinder in the contact zone. This is set in such a way that a specific length s , of the hard sheath of the cylinder penetrates into the flexible cylinder. This length s (usually 0.10 mm) is called metric pressure. Since the existence of the rigid bearer rings at the cylinder ends prevents the reduction of the centre distance between the same, the surfaces of blanket and printing plate can be raised to a higher level compared

to the bearers for increasing the squeeze. This is usually referred to as blanket projection \dot{U}_G and plate projection \dot{U}_P , respectively.

$$s = \ddot{U}_G + \ddot{U}_P \quad \{1\}$$

The metric pressure in the range of $s = 0.10$ mm can be calculated and adjusted with the help of equation {1} with any number of the pair of values: \ddot{U}_G, \ddot{U}_P .

The condition $\ddot{U}_G = \ddot{U}_P = s / 2$ is obvious for a pair of cylinders with equal bearer diameters. Similarly to above, the blanket cylinder and plate cylinder along with the overlying offset plate have the same diameter. Hence it would be expected that there exists no slip between the two. However, according to the tests, this is not true. The existence of a measurable slip when passing through the contact zone can be explained geometrically as follows.

Each point on the plate surface relative to the blanket cylinder surface traces a defined rolling curve, referred to as an epicycloid [2]. Since each point on the plate surface \ddot{U}_P , is located around the outside of the rolling circle (i.e. the bearer ring), it traces an extended epicycloid. Figure 5 shows an example of the mentioned curve.

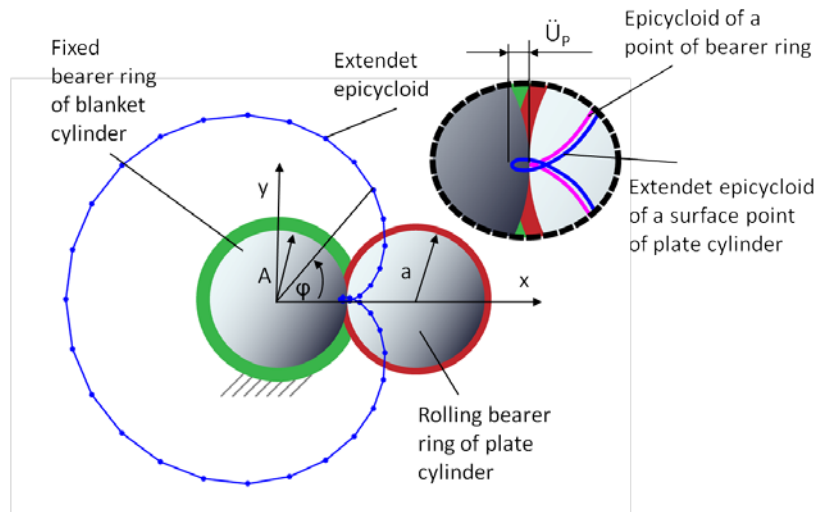


Figure 5 – Extended epicycloid

It is worth noting that the extended epicycloid in the region of the fixed cylinder describes a loop. This interesting characteristic will be analyzed below in further detail. The equation in parametric form for the extended epicycloids is [2]:

$$y = (A+a) \sin\varphi - \lambda a \sin((A+a)/a)\varphi \quad \{2\}$$

- A ... radius of the cylinder
- a ... radius of the rolling circle
- φ ... angle of rotation
- $\lambda = (a + \ddot{U}_P)/a$

The extended epicycloids calculated for the machine GTO52 (Heidelberg) and LaborMAN (manroland) is shown below. The printing couples of these machines are shown schematically for GTO in Fig. 6 and for LaborMAN in Fig.1.

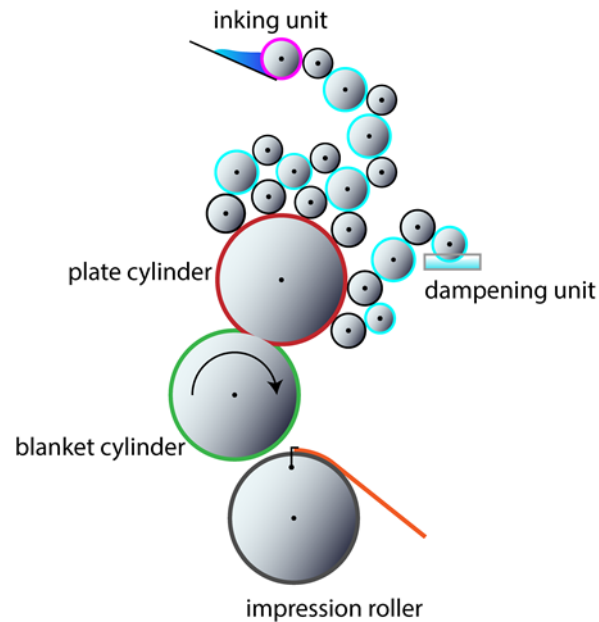


Figure 6 – Schematic of the printing unit of the sheet-fed offset press GTO52 from Heidelberger Druckmaschinen AG

The bearer ring radius of the blanket and the plate cylinder of the machine GTO52 is $R = 90 \text{ mm}$, the metric pressure is $s = 0.10 \text{ mm}$.

The plate projection, \dot{U}_p accordance with the condition is initially adopted to be $\dot{U}_p = 0.05 \text{ mm}$. The equation of the extended epicycloid with $A = a = R$ and $\lambda a = R + \dot{U}_p$ is of the form

$$\begin{aligned} x &= 180\cos\varphi - 90,05\cos2\varphi \\ y &= 180\sin\varphi - 90,05\sin2\varphi \end{aligned} \quad \{3\}$$

A magnified view of the epicycloid in the range of $-5^\circ \leq \varphi \leq 5^\circ$ is shown in Figure 7 to clearly illustrate the movement conditions at the contact zone.

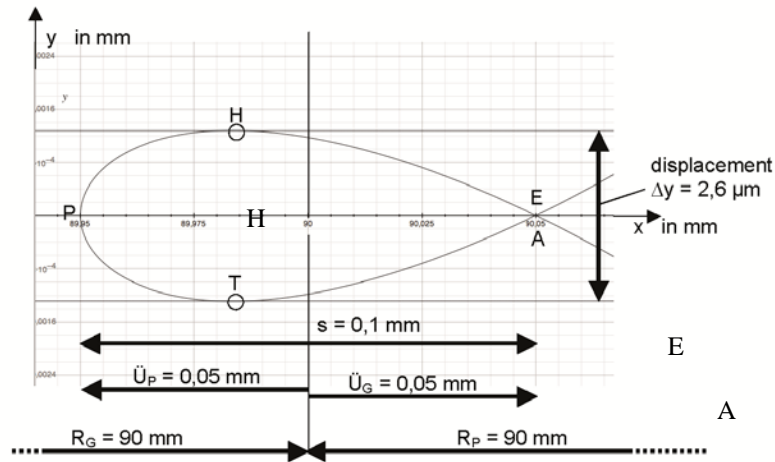


Figure 7 – Extract of the extended epicycloid for GTO shown in Fig.8 in range of $-5^\circ \leq \varphi \leq 5^\circ$,
 R_G ...bearer radius of the blanket cylinder,
 R_P ...bearer radius of the plate cylinder,
 s ...metric pressure between plate and blanket cylinders,
 \ddot{U}_G ...projection of blanket cylinder,
 \ddot{U}_P ...projection of plate cylinder,
A ...start of contact between the plate surface and t blanket surface,
E ...end of contact

Running at an angle of rotation φ , the considered point on the plate surface contacts the rubber blanket at point A. Here, it is pressed under pressure in the rubber blanket and experiences both a radial push in x-direction and, at the same time moves in y-direction, i.e., tangentially to the blanket cylinder, thereby forming an epicycloid. It can be assumed that the movement in y-direction is due to the lateral dimensional stability of the top layer from the rubber blanket, thereby causing a slip of the considered point on the plate by the radially indented blanket surface. This process continues until the observed point on the plate surface leaves the contact area with the blanket at point E. The extended epicycloid therefore describes for each angle φ in the contact zone, a radial pressure and tangential displacement according to magnitude and directionality respectively. Fig. 8 and 9, show a recorded diagram of the components as a function of movement of the angle of rotation $x = x(\varphi)$ and $y = y(\varphi)$. It is worth noting that despite the same position of the points A and E in the epicycloid (Fig. 5), a longitudinal displacement Δy occurs (Fig. 9).

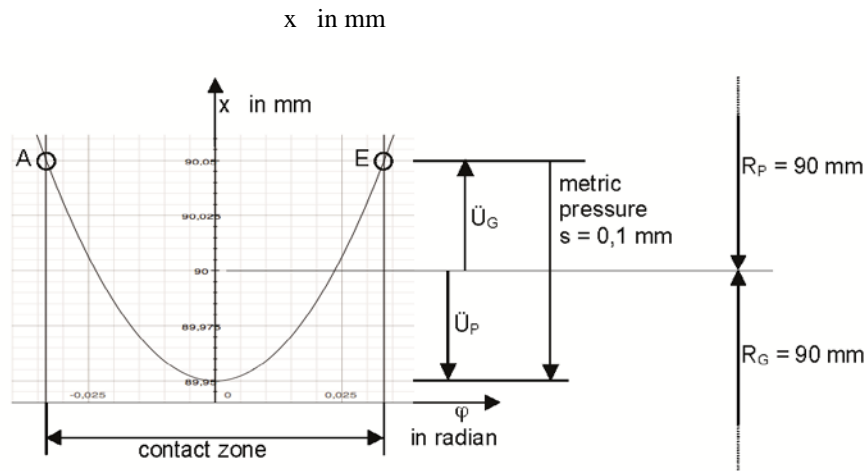


Figure 8 – Pressure profile within the zone of contact (GTO)

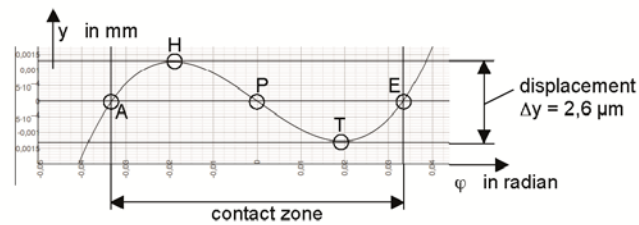


Figure 9 – Displacement curve within the zone of contact (GTO)

The displacement curve $y = y(\varphi)$ shows that immediately after contact of the point on the plate surface with the blanket at point A, there is an increasing shift in the positive y-direction, i.e. in printing direction. This is followed by an inversion in the displacement that starts at H and goes till T in the negative y-direction, i.e. opposite to the direction of printing. Finally, from T to E, which is the end of the zone of contact, a shift occurs again in the positive y-direction. The amount of displacement at the plate (carrying the ink) – blanket nip, presumably due to the lateral movement of top layer of blanket causes an elongation of the printed image in the printing direction by precisely this value. Furthermore, this movement indicates a tribological abrasion process that can wear the plate and rubber blanket. Thus, there are several reasons to keep this abrasive motion as small as possible. Solutions for minimizing the amount of displacement have been presented, as will be shown later. However, the complete elimination of the shift while maintaining a metric pressure is not possible because the existence of pressure is the basic technical requirement for ink transfer in a classical offset printing process.

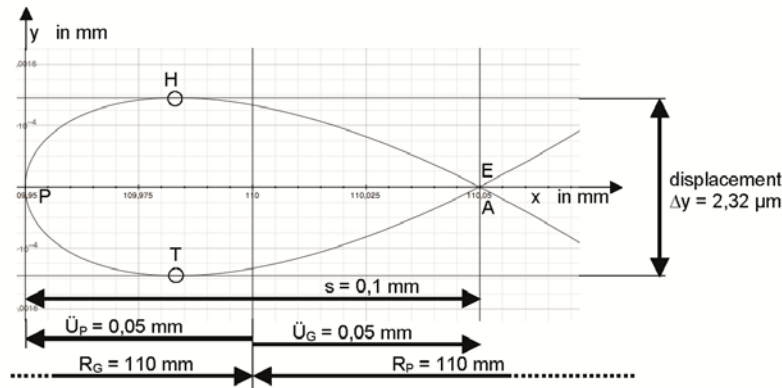
The Fig. 5, 8 and 9 open up yet another perspective on the processes taking place in the contact zone. They depict not only the relation of the rotational angle and the ongoing motion of a point on the plate surface through the described zone, but simultaneously provide a picture of the complete scenario involving the movement occurring through it. This perspective also enables us to draw conclusions on the shear stress situations in this region.

Although in contrast to Heidelberg GTO 52, LaborMAN web offset press is not equipped with bearer rings, the electronically controlled direct drive of the print cylinders operates at a high level of precision. The measured difference in the angle of rotation of the cylinders to each other evaluated on the circumference was very low value with $1\mu\text{m}$. The lack of bearer rings is therefore practically balanced.

The radii of the cylinders (comparable to radii of the bearer rings) have a size of $R_G = R_P = 110\text{ mm}$. The metric pressure/squeeze is $s = 0.10\text{ mm}$, which is generated by, \ddot{U}_G and \ddot{U}_P , for instance $\ddot{U}_P = \ddot{U}_G = 0.05\text{ mm}$. With these initial values, the extended epicycloid of a point on the plate surface has the following equation:

$$\begin{aligned} x &= 220\cos\varphi - 110,05\cos2\varphi \\ y &= 220\sin\varphi - 110,05\sin2\varphi \end{aligned} \quad \{4\}$$

In the contact zone between plate and blanket cylinder, the extended epicycloid has the shape as shown in Fig. 10



The displacement Δy , which is the distance between the points H and T is, $\Delta y = 2.32\ \mu\text{m}$.

Variation and Optimization

The handbook of LaborMAN depicts different values for the under projection, which are $\ddot{U}_P = 0.02\text{ mm}$ and $\ddot{U}_G = 0.10\text{ mm}$ [4]. Fig. 11 shows the extended epicycloids generated using the handbook values in contrast to Fig. 10. Values used were $\ddot{U}_P = 0.02\text{ mm}$ for handbook value and other extended epicycloids with $\ddot{U}_P = 0.060\text{ mm}$ and $\ddot{U}_P = 0.045\text{ mm}$. In each case, the metric pressure of $s = 0.120\text{ mm}$ – as described in the handbook - has been kept constant and marked.

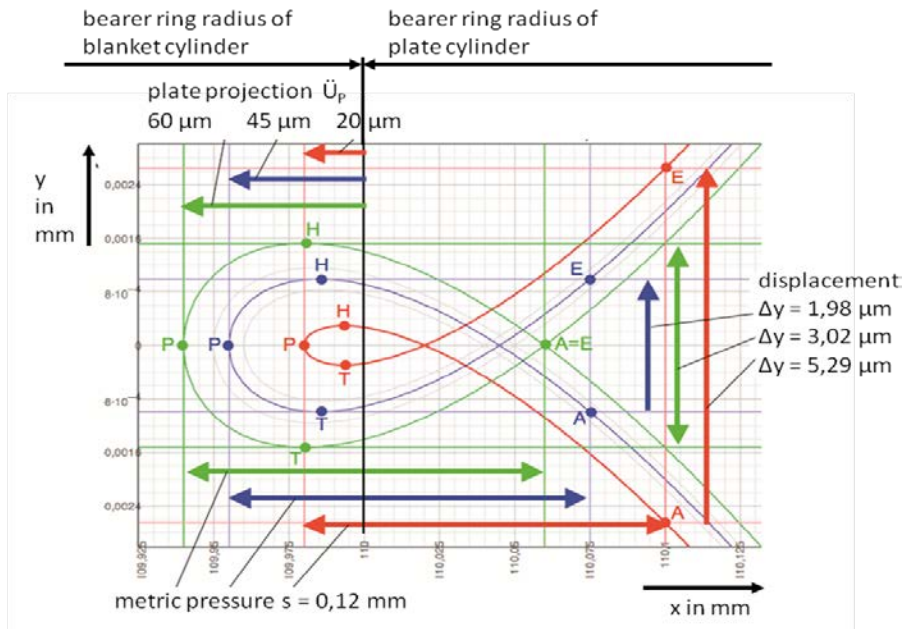


Figure 11 – Extended epicycloids with different parameters

It turns out that in contrast to the curve seen in Fig. 10, the points *H* and *T* on the epicycloid are closer together when the press is adjusted according to the handbook, while the points *A* and *E* are much further apart. As the plate contacts the printing blanket at point *A*, where the ink transfer from plate to blanket begins and plate and blanket remain in contact till point *E*, the distance between *A* and *E* is relevant to us. Therefore it is clear, that a variation of values \ddot{U}_p and \ddot{U}_G can significantly reduce the distance between points *H* and *T* but the same time increase the distance between the points *A* and *E*.

Minimum displacement can be achieved when the two distances are the same. In Fig. 11, the pair of values was calculated with iterations that satisfy this condition and thus result in the smallest possible shift.

Hence, the theoretical shift of Δy could be reduced from $\Delta y = 5.29 \mu\text{m}$ to $\Delta y = 1.98 \mu\text{m}$. To which extent this theoretical displacement length is measurable in practice with printing tests on the machine LaborMAN, is documented in the next section, “Verification through print trials”.

Total Displacement in the Printing Unit

cylinder can be assumed to be rigid, since the paper with a thickness p , where $p = 0.07$ mm (for instance) after compression is only $\Delta p = p / 1000 = 0.07 / 1000 = 0.00007$ mm thinner. Compared to the compression of the blanket of $s = 0.1$ mm = $100 \mu\text{m}$, this small amount of $0.07 \mu\text{m}$ is quite negligible. Therefore the contact zone between blanket and impression cylinder is analogous to the contact zone between plate and blanket cylinder and is exposed to similar displacement conditions. Since it is the same rubber blanket cylinder in both cases, the \ddot{U}_G parameters from the first contact zone are already preset and not selectable. Taking into account the required metric pressure s , adjustment of paper is carried out by $\ddot{U}_D = s - \ddot{U}_G$. This relationship between the parameters restricts the scope for a minimization of the total displacement.

The total displacement occurring in the printing unit, Δy_{gesamt} is the sum of displacement in the contact zone between the plate and blanket cylinder Δy_{P-G} and between blanket and impression cylinder Δy_{G-D} .

Fig. 12 shows the extended epicycloids for the contact zone between plate cylinder and blanket cylinder.

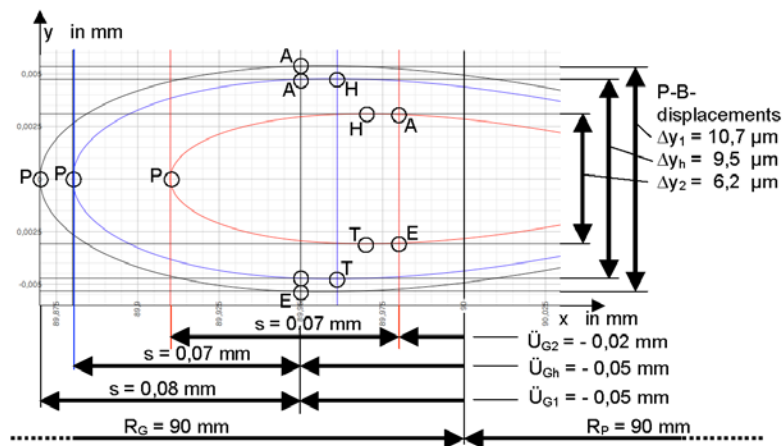


Figure 12 – Extended epicycloids for the contact zone between plate and blanket cylinders with $\ddot{U}_{P1} = 0.09$ mm, $\ddot{U}_{Ph} = 0.12$ mm, $\ddot{U}_{P2} = 0.13$ mm. Subscript h relates to the settings according to the handbook of the GTO 52 printing press

In Fig. 13, the extended epicycloids are plotted for the contact zone between the blanket cylinder and the impression cylinder which relate to the settings with the subscripts 1 , h and 2 (cf. Fig. 14). Subscript h relates to the settings according to the handbook of the GTO 52 printing press.

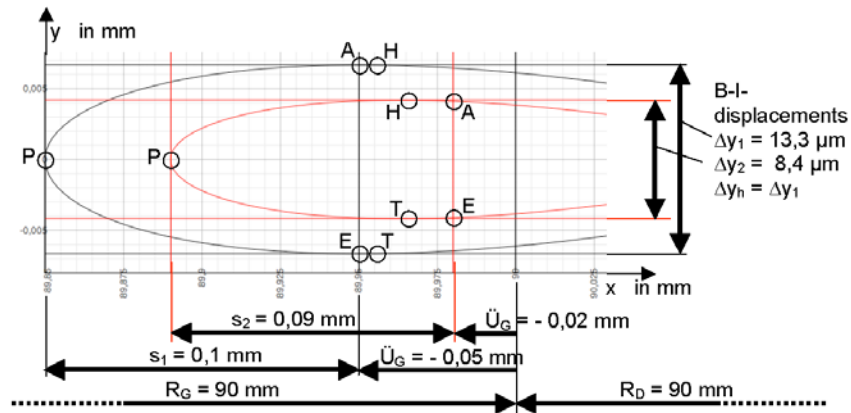


Figure13 – Extended epicycloids for the contact zone between blanket and impression cylinder with paper between the nip
 $\ddot{U}_{D1} = \ddot{U}_{Dh} = 0.15 \text{ mm}$, $\ddot{U}_{D2} = 0.11 \text{ mm}$

The total calculated displacements in the printing unit of GTO52 Δy_{gesamt} is summarized in Table 1. The total displacement is the sum of the shift amounts that occur in the contact zone between plate cylinder and blanket cylinder Δy_{P-G} and in the contact zone between blanket and impression cylinder Δy_{G-D} .

$$\Delta y_{gesamt} = \Delta y_{P-G} + \Delta y_{G-D} \quad \{5\}$$

	Handbook parameters	Experiment 1	Experiment 2
Δy_{P-G}	9.5 μm	10.7 μm	6.2 μm
Δy_{G-D}	13.3 μm	13.3 μm	8.4 μm
Δy_{gesamt}	22.8 μm	24.0 μm	14.6 μm

Table 1 – Calculated displacements Δy in printing unit of GTO52

To check to what extent the calculated shift lengths can be detected on the printed product, printing tests on the LaborMAN and GTO52 were carried out.

VERIFICATION THROUGH PRINT TRIALS

For the printING tests on the LaborMAN, the following settings were taken:

- $\ddot{U}_P = 0.14 \text{ mm}$, $\ddot{U}_G = -0.2 \text{ mm}$ („Extreme“)
- $\ddot{U}_P = 0.02 \text{ mm}$, $\ddot{U}_G = 0.05 \text{ mm}$ („Normal“)

The extended epicycloids for both cases are plotted in FiG: 14

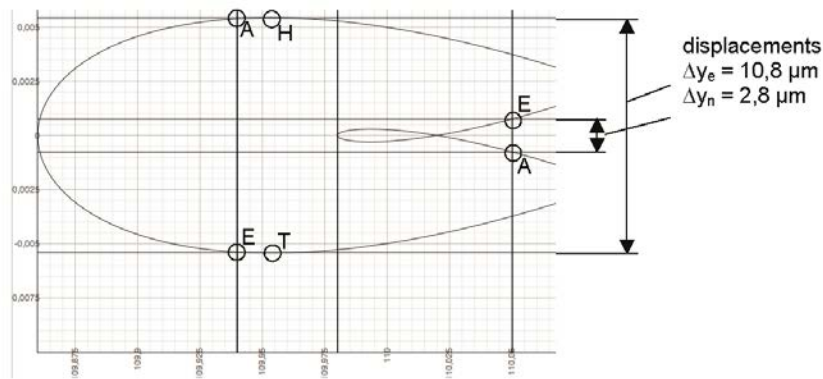


Figure 14 – Extended epicycloids for the test settings "normal" and "extreme" for the LaborMAN

With both settings trial prints were produced in small print runs. The print samples were measured with regard to elongation of the printing elements. In order to measure the elongation of printing elements in the longitudinal direction, a test printing plate was used which incorporated regularly arranged transverse pressure bars of same width over the entire length. The test printing form with these transverse bars, the so-called shift areas is illustrated in Fig. 15.

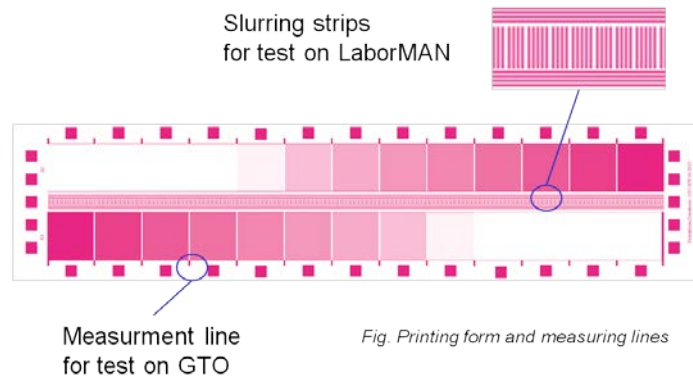


Figure 15 – Test printing plate for printing tests on LaborMAN and GTO

The edges of the bars were somewhat wavy and the elongation could not be accurately measured because of these unsharp edges. However, when viewed at ten times magnification under the microscope, the printed element was quite clearly visible with a definite edge and therefore measurement could be applied with good reproducibility at the edges of the bar. The measured width of each slurring strip varied between 210 and 230 micrometers. It could be determined with an accuracy of less than one-fiftieth of the measuring scale.

Using the same measuring method, the width of each bar on the printing plate was measured for comparison purposes. The measured widths of the bars on the printed product were considerably larger than the measurements obtained on the printing plate. The reason for this could be the press itself and not just the slippage due to the displacement as mentioned before. Other causes include the characteristic process that occurs in the offset printing process, i.e. dot gain or tonal value increase, broadening the printing elements. To ensure this occurred due to the slip at the contact zones, sample sheets printed during two different print tests with different slip settings were compared. This was carried out by changing the relation between \ddot{U}_p and \ddot{U}_G . The two editions were printed in immediate succession to prevent any other possible influences. From the differences measured in the width of the bars, conclusions could be drawn in accordance with the theoretically determined differences in width.

Fig. 16 [FUE11] shows the measurement results under both conditions.

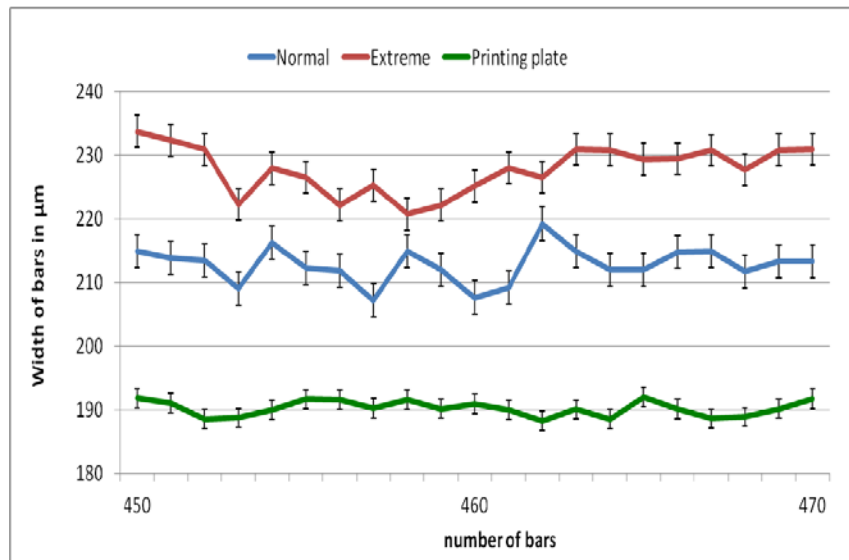


Figure 16 – Chart comparing the measured width of slurring strips from two test print runs obtained with same nip pressure but different $\ddot{U}_p - \ddot{U}_G$

The theoretically determined displacement lengths for both settings are shown in Fig. 14. The calculated difference of displacement $\Delta\Delta y$ between the two settings was $\Delta\Delta y = \Delta y_e - \Delta y_n = 10.8 \mu\text{m} - 2.8 \mu\text{m} = 8 \mu\text{m}$. The highest values for the shift were measured from the print test with ‘extreme’ settings. Fig. 16 shows that the obtained measurement values of displacement lie in the vicinity of the theoretically calculated values.

This result can be considered as a first confirmation of the validity of the theoretical calculations including the idealized geometric assumptions. Causes for the deviations in the measured results of the calculations can be enlisted as:

- Bearing clearance in the printing unit,
- Tolerances of metric pressure during adjustment,
- Thickness tolerances of the blanket, the offset plate, the packing foil,
- Measurement error in the analysis of the prints

Further printing test at the LaborMAN with different settings as well as on other machines, especially industrial presses, would help to summarize the degree of compliance between the calculated and practical results. This would also help to evaluate the legitimacy of construction and the degree of precision required for the measurements in practical environment.

In order to further investigate the validity of the calculations in practical scenario, another set of experiments was conducted. On the one hand, a different printing press was used: the Heidelberg GTO 52, and, on the other hand, the slip calculation was extended to the entire printing mechanism. In addition to the contact zone between plate and blanket cylinder, the second contact zone of an offset printing unit was included in the calculation. That is, the zone between blanket and impression cylinder with the printing paper sandwiched in between. The equations used have been described above.

Printing Tests Conducted on GTO52

For the second print tests, settings of $\ddot{U}_P = 0.09$ mm, $\ddot{U}_G = - 0.02$ mm and $\ddot{U}_D = 0.11$ mm were adopted.

Fig. 17 shows the schematic representations of the utilized settings, including the cylinder bearers, material thicknesses and thickness projection composition for both test print runs.

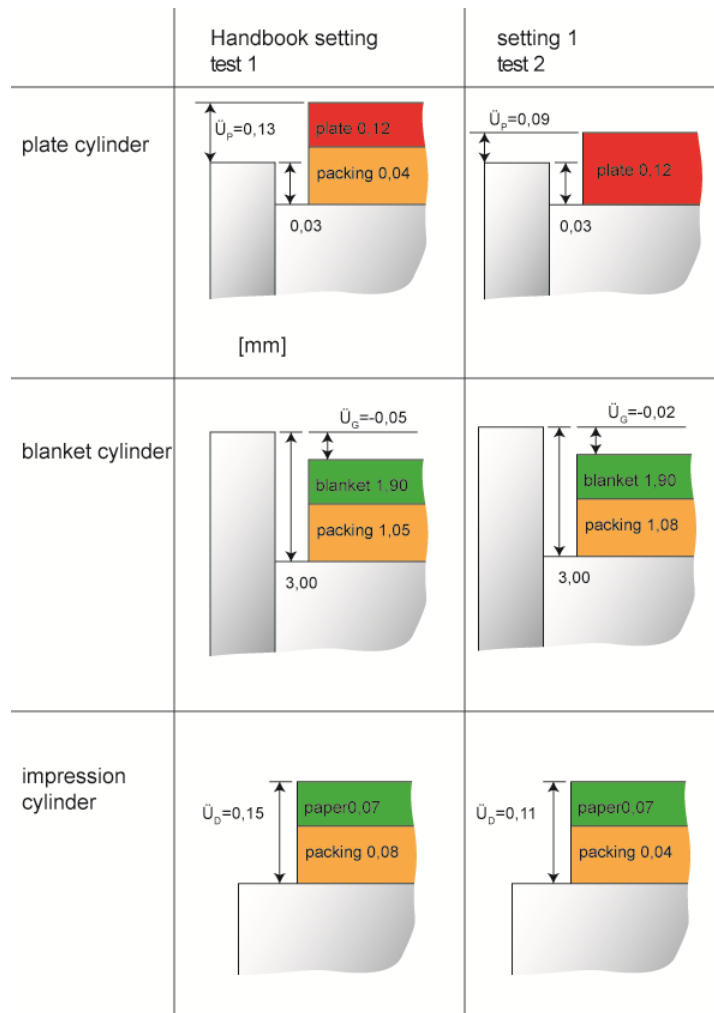


Figure 17 – Overview of settings: undercuts, bearer rings, material thickness, projection thicknesses, \dot{U}_p , \dot{U}_g , \dot{U}_d

The subject of the test chart is represented by Fig. 15. A property of the Mitsubishi printing plate, enabled also to avoid inaccurate contours of the slip bar occurring due to exposure and developing procedure, were undesirable for the intended tests. Much sharper and straighter edges of the bars were obtained on the test prints measuring about 0.7 mm wide and 2.7 mm long, arranged laterally between the raster surfaces. The measurement of the bar width under the microscope showed a measurement uncertainty in the order of 5 μm . Therefore a sufficiently reliable statement can be made from the measured width differences of these bars. The results are presented in Fig. 18.



Figure 18 – Measurement lines under microscope on bars (printed element)

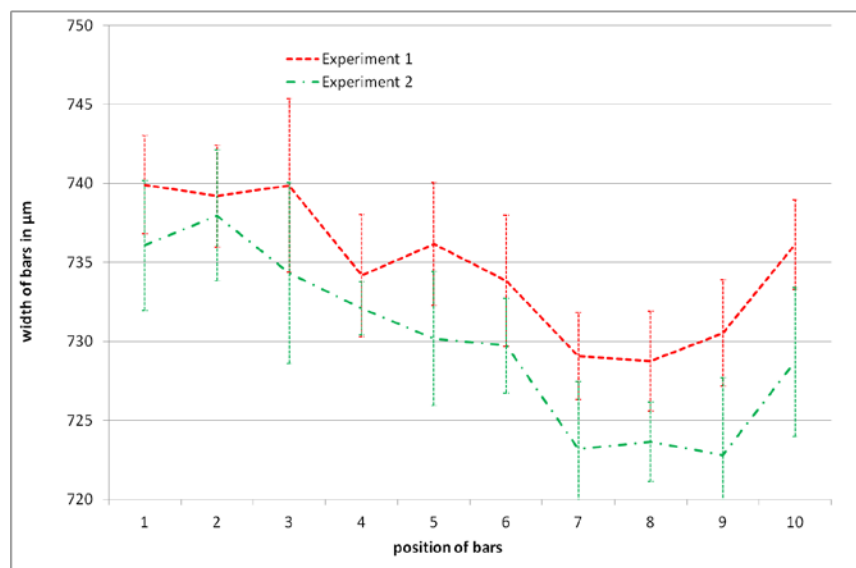


Figure 19 – Measurement of width of the bar printed under two conditions with different settings

Comparison with the Calculated Results

The measurement results permit the comparison of the width of each of the bars. Each of the two series of measurements when superimposed show a sinusoidal variation along the measuring point 1 to 10, i.e., along the entire length of the test chart, indicating a systematic error. The cause for this error still has to be analysed in detail. However, it could be linked to the existence of a slight eccentricity between the cylinder jacket and bearer in each of the two cylinder pairs. However, it has no significance for the results obtained from evaluation of the displacement. A distinctive observation of the printed result is the clear identification of the size difference between the bars from experiment 1 and the bigger (wider) bars from experiment 2. Thus, the displacement or shift from the printing unit is greater in the experiment 2 as in experiment 1, which is consistent with the calculations.

Comparing the values, the measured difference lies between 1.3 μm and 7.9 μm while the theoretically calculated was value 9.4 μm.

Reasons for the measured values being lower than the calculated ones are:

- In the proximity of the points *A* and *E*, the pressures are very low and insufficient for proper ink transfer. Therefore, the displacement in these areas is not completely visible on the printed product and thus the lower measurement value results.
- Ink transfer in the contact zone between blanket and paper is even less, since the ink layer thickness is about half of that between plate and blanket. In addition, the solvent taken up by the paper further hinders the process. This also contributes to lowering of the measured values.
- The elastic recovery of the blanket from the indented or compressed state to the normal state is a time-dependent material constant. If the speed of separation of the two surfaces at the outgoing nip is greater than the elastic recovery speed of the rubber blanket, a premature lifting of the two surfaces occurs. This causes the point *E* to shift back. The displacement is smaller.

The presented method allows calculation of

- displacements occurring at the nip in offset printing,
- minimization of the theoretical displacements

in order to improve the printing quality. An even more significant outcome is the reduction of wear of printing plates and blankets. This should be investigated with the help of long-term tests on industrial printing presses.

ACKNOWLEDGEMENT

This paper was developed in the course of the cooperation project "Surface-modified offset blankets" funded by the AIF and carried out by Weros Technology GmbH, Melle, Germany, and the Professorship Print Media Technology (pmTUC) of Chemnitz University of Technology, Chemnitz, Germany.

REFERENCES

1. Hofmann, P. and Liebau, D., "Beitrag zur Untersuchung des dynamischen Verhaltens von Druckwerken in Rollenoffset-Rotationsmaschinen," Dissertation Technische Hochschule Karl-Marx-Stadt 1969, S. 86.
2. Bronstein, I.N., Semendjajew, K.A.: Taschenbuch der Mathematik, Verlag Harri Deutsch, 2012, ISBN 978-3-81712-018-5.
3. Handbuch zur Labordruckmaschine LaborMAN.
4. Fügmann, U. and Beier, W., Proceedings zum 11. Bahnlaufseminar 2011: Förderverhalten einer Hart-Weich-Walzenpaarung, Verlag für Wissenschaft und Forschung, 2013, ISBN 978-3-89700-195-4.
5. Phoenix, Gummituchprospekt.
6. Johnson, K.L., Contact Mechanics, Cambridge University Press, 2003, ISBN 0 521 34796 3, S. 246 ff.
7. Volmer, J., Getriebetechnik, 1995, Verlag Technik ISBN 978-3-3410 1-137-9.
8. Helbig, T. and Bosse, R., Druckqualität, Grundlagen der Qualitätsbewertung im Offsetdruck Druckqualität, Polygraph Verlag Frankfurt am Main, 1993, ISBN 978-3-93493-820-5.

9. Kipphan, H., Handbuch der Printmedien, Springer Verlag, 2000, ISBN 978-3-54066-941-8.
10. Teschner, H., Druck & Medien Technik, 11. Auflage, Fachschriften Verlag, 2003 ISBN 3-931436-88-8 S.13.32.
11. Walenski, W., Das Papierbuch, Verlag Beruf und Schule 1999, ISBN 978-3-8801-584-0.